

Serial Assessment of Vessel Interactions After Drug-Eluting Stent Implantation in Unprotected Distal Left Main Coronary Artery Disease Using Frequency-Domain Optical Coherence Tomography

Yusuke Fujino, MD^{1,2*}, Guilherme F. Attizzani, MD^{1*}, Hiram G. Bezerra, MD, PhD¹, Wei Wang, PhD¹, Satoko Tahara, MD, PhD², Hirosada Yamamoto, MD¹, Daniel Chamie, MD¹, Tomoaki Kanaya, MD¹, Emile Mehanna, MD¹, Kensuke Takagi, MD², Sunao Nakamura, MD, PhD² and Marco A. Costa, MD, PhD¹

Total word count: 4937

Brief title: ULM response after DES implantation by FD-OCT

*: authors contributed equally to this study.

From the ¹Harrington Heart and Vascular Institute, University Hospitals Case Medical Center, Case Western Reserve University, Cleveland, Ohio; and the ² Department of Cardiology, New Tokyo Hospital, Chiba, Japan

Address for correspondence:

Marco A. Costa, M.D., Ph.D., FSCAI, FACC.

Professor of Medicine, Case Western Reserve University

Harrington Heart and Vascular Institute
University Hospitals Case Medical Center
Case Western Reserve University
11100 Euclid Avenue
Cleveland, Ohio 44106
Tel.: (216) 983-5887
Fax: (216) 844-8318
Email: marco.costa@uhhospitals.org

Disclosures: Dr. Bezerra has received honoraria grants from St. Jude Medical, Inc, Dr. Costa is on the Speakers' Bureaus of and is a consultant for Daiichi-Sankyo, St. Jude, Boston Scientific Corporation, Sanofi-Aventis, Eli Lilly, and Medtronic; he is also on the Speakers' Bureaus of and is a member of the Scientific Advisory Boards for Abbott, Cordis, St Jude Medical, Inc, and Scitech. Guilherme F. Attizzani has received consultant honoraria from St Jude Medical, Inc. All other authors have reported that they have no relationships to disclose.

ABSTRACT

Objective: We aim to assess stent-vessel interactions after drug-eluting stent (DES) implantation in unprotected left main coronary artery (ULM) by frequency-domain optical coherence tomography (FD-OCT).

Background: Percutaneous coronary intervention (PCI) using DES in ULM has been increasingly performed in routine practice. Recently, FD-OCT assessments of DES-vessel interactions have been used as surrogates for DES safety; however, there are no FD-OCT studies in ULM.

Methods: We prospectively enrolled 33 consecutive patients with ULM disease treated with sirolimus- (n=11) and everolimus-eluting stents (n=22). FD-OCT assessments were performed post-PCI and at 9-month follow-up. Three different segments of ULM were compared: distal (DIS), bifurcation (BIF), and ostial-body (BODY). The primary endpoints were percentage of uncovered and malapposed struts at 9-month follow-up, and the secondary endpoint was neointimal hyperplasia (NIH) area.

Results: We analyzed 25,873 stent struts. Significant differences were demonstrated for percentage of uncovered struts (3.4%, 11.7%, and 18.7%, respectively for DIS, BIF, and BODY, $p < 0.05$ for all the comparisons). Malapposition was also more common in BODY (5.3%) compared with DIS (0.6%), and BIF (2.0%) segments ($p < 0.05$ for BODY vs. DIS, and BODY vs. BIF). Equivalent NIH areas were demonstrated in all segments. Acute malapposition rates led to different patterns of DES-vessel interactions at 9-month follow-up.

Conclusion: Distinct patterns of DES-vessel interactions were demonstrated in different segments of ULM. Acute stent strut malapposition impacts these findings.

Key Words: Frequency-domain optical coherence tomography; unprotected left main coronary artery disease; percutaneous coronary intervention

Condensed Abstract:

Frequency-domain optical coherence tomography (FD-OCT) assessments have been used as surrogates for drug-eluting stent (DES) safety; however, there are no FD-OCT studies in unprotected left main coronary artery (ULM). We prospectively enrolled 33 consecutive patients with ULM disease involving distal bifurcation. FD-OCT assessments were performed post-PCI and at 9-month follow-up, and three different segments of ULM were compared: distal (DIS), bifurcation (BIF), and ostial-body (BODY). While BODY segment showed more uncovered and malapposed struts, NIH area was equivalent between segments. In addition, acute malapposition led to an impact in DES-vessel interactions at 9-month follow-up

Abbreviations and acronyms:

BIF = bifurcation

BODY = ostial-body

DES = drug-eluting stents

DIS = distal

EES = everolimus-eluting stents

FD-OCT = frequency-domain optical coherence tomography

GEE = generalized estimating equations

ISR = in-stent restenosis

NIH = neointimal hyperplasia

SES = sirolimus-eluting stents

SIT = strut-level intimal thickness

ST = stent thrombosis

ULM = unprotected left main coronary artery

Introduction

Indications of percutaneous coronary intervention (PCI) using drug-eluting stents (DES) for unprotected left main coronary artery (ULM) disease are increasing worldwide (1-3). However, safety concerns regarding DES are amplified in ULM due to the large amount of myocardium at risk (4). Intravascular optical coherence tomography (OCT) has been extensively validated against histology (5), and is currently used as surrogate for in vivo healing assessment after DES implantation in clinical trials (6). OCT studies have provided invaluable insights into vascular reactions to stents (7, 8, 9), making this technology an attractive tool to investigate DES interactions in the setting of ULM PCI. Compared with prior generation time-domain OCT system, the latest frequency-domain OCT (FD-OCT) has increased pullback speed (up to 25mm/s), obviating the need for proximal balloon occlusion during image acquisition, and provides a larger field of view (~10mm), enabling evaluation of large vessels. We, therefore, performed a comprehensive evaluation of acute and late DES-vessel interactions of lesions involving ULM distal bifurcation using serial FD-OCT imaging.

Methods

Study population. A total of 54 consecutive patients underwent PCI with DES in ULM from March 2010 to September 2010 and 33 fulfilled the inclusion criteria to be enrolled in this prospective single center (New Tokyo Hospital, Chiba, Japan) study. Patients treated by single stent strategy with crossover from ULM to left anterior descending coronary artery (LAD) were eligible if they had de novo obstructive atherosclerotic disease in ULM related to myocardial ischemia or stenosis >50% by angiographic assessment. Exclusion criteria included congestive heart failure with left ventricle ejection fraction <30%, ST-segment elevation myocardial infarction, chronic kidney disease (serum creatinine>1.5 mg/dl) not on hemodialysis, inability to comply with follow-up requirements, known allergy to antiplatelet agents or contrast dye and life expectancy <1 year. Patients treated with two stents strategy (culotte, crush, mini crush)

were also excluded. FD-OCT was performed in all patients post-PCI and at 9-month follow-up. The study protocol was approved by the institutional review board and informed consent was obtained for every patient before any intervention was performed.

PCI procedure. All patients were treated with aspirin (200mg loading-dose) and clopidogrel (300mg loading-dose) at least 24 hrs before PCI. After stent implantation, aspirin was maintained indefinitely (200mg/day), while clopidogrel (75mg/day) was continued for at least 1 year. Cilostazol was also prescribed at least 3 months post-PCI (10). All patients received an intra-arterial bolus injection of 6,000-10,000 IU of heparin and intracoronary isosorbide dinitrate (2-3 mg) before initial angiography. PCI was performed by femoral or radial approaches using 6- or 7-F guiding catheters. Sirolimus-eluting (SES, Cypher, Cordis, Miami Lakes, Florida) or everolimus-eluting stents (EES, XIENCE V, Abbott Vascular, Santa Clara, California and PROMUS, Boston Scientific, Natick, Massachusetts) were implanted per operator's discretion with cross over single stent strategy. PCI success was defined when <20% residual stenosis with normal distal blood flow (TIMI 3) was achieved. Procedural success was defined as PCI success without any in-hospital adverse events.

Quantitative coronary angiography (QCA) analysis. QCA was performed pre-, post-PCI and at 9-month follow-up. Angiographic measurements were made in two matched orthogonal projections. Offline analyses of digital coronary angiograms (CASSII, Pie-Medical, Maastricht, The Netherlands) were performed by an independent core laboratory (Cardiovascular Imaging Core Laboratory, University Hospitals Case Medical Center, Cleveland, Ohio) using validated quantitative methods (11).

FD-OCT image acquisition and analysis. A conventional angioplasty guidewire (0.014-inch) was advanced distal to the region of interest, then the 2.7 French FD-OCT catheter (Dragonfly™, St Jude Medical, St Paul, Minnesota, USA) was advanced over the guidewire at least 10-mm beyond the region of interest. The images were calibrated by automated adjustment of the Z-offset and automated pullback was set at 20mm/s. Data were acquired using a

commercially available FD-OCT system (C7-XR™, OCT Imaging System, St Jude Medical, St. Paul, Minnesota, USA) after intracoronary administration of 50-200µm of nitroglycerin through conventional guiding catheters and digitally stored. During imaging acquisition, blood was displaced by injection of isosmolar contrast dye (100%) with a power injector. FD-OCT pullbacks were performed from LAD to the ostial-body part of ULM. Image acquisition was performed in a similar fashion post-PCI and at 9-month follow-up. An independent core laboratory (Cardiovascular Imaging Core Laboratory, Harrington Heart and Vascular Institute, University Hospitals, Case Medical Center, Cleveland, OH) reviewed all FD-OCT images. The images were analyzed by 2 independent investigators blinded to the angiographic and clinical data. FD-OCT analyses were performed using dedicated software with an automated contour-detection algorithm (Off-line Review Software, version C.0.2; St Jude Medical, St Paul, Minnesota, USA). Commercially available dedicated software (Amira 5.4.2, Visage Imaging, San Diego, CA, USA) was used for three-dimensional reconstruction of FD-OCT two-dimensional images. Only single stents crossover from ULM ostial-body to LAD were analyzed. Aiming at obtaining a comprehensive analysis, ULM was divided into three major segments, as follows: ostial-body (BODY), bifurcation (BIF), and distal (DIS) (Figure 1). All cross-sectional images were initially screened for quality assessment and excluded from analysis if any portion of the stent was out of the screen, if a side branch (except ULM bifurcation) occupied $>45^\circ$ of the cross-section, or if the image had poor quality caused by residual blood, artifact, or reverberation (12). Qualitative image assessment was performed in every frame, while quantitative measurements were performed every 2 frames (i.e., every 0.4-mm) (13) along the entire stented segment. In BIF segment, cross-sections were analyzed as previously described (14) Strut-level intimal thickness (SIT) was determined based on automated measurements performed from the center of the luminal surface of each strut blooming and its distance to the lumen contour (12). Struts covered by tissue had positive SIT values, whereas uncovered or malapposed struts had negative SIT. Strut malapposition was

defined when the negative value of SIT was higher than the sum of strut thickness plus abluminal polymer thickness, according to stent manufacturer specifications, plus a compensation factor of 20 μ m to correct for strut blooming (9,13). Tissue protrusion was defined as a tissue prolapse between stent struts that directly correlates with the underlying plaque, without abrupt transition and different optical properties (14). Presence of thrombus and dissections were determined as previously described (15, 16). Stent imaging completeness was defined when stent struts were observed in at least 3 quadrants at each major segment. FD-OCT derived malapposition values were obtained by means of 360° chords, distributed between the lumen and stent contours. The term “DES-vessel interactions” comprises acute modifications induced by DES implantation in either vessel or stent (i.e., tissue protrusion, acute malapposition), as well as 9-month follow-up FD-OCT surrogates for vessel healing response (i.e., stent strut coverage, NIH, malapposition).

In order to assess the impact of stent strut malapposition post-PCI (acute stent strut malapposition) in DES-vessel interactions at 9-month follow-up, FD-OCT pullbacks were aligned based on fiduciary points (distal stent edge, branches, and calcifications) and the major segments (i.e. BODY, BIF, and DIS) along the stented segment were automatically sub-segmented in 2.5-mm intervals (sub-segments) (8). The median percentage of stent strut malapposition post-PCI for each of the major segments was used as reference: sub-segments with rates of malapposition that were lower than the reference value for that specific major segment were labeled as the “Low” (percentage of acute malapposition) group, whereas sub-segments with percentages of malapposition higher than the median value were labeled as the “High” (percentage of acute malapposition) group.

Endpoints. The primary endpoints were the percentage of uncovered and malapposed stent struts assessed by FD-OCT at 9-month follow-up in different segments (BODY/BIF/DIS). The secondary endpoint was neointimal hyperplasia (NIH) area at 9-month follow-up in each segment. The impact of the percentage of malapposed stent struts post-PCI in vascular response

at 9-month follow-up was also evaluated. Major adverse cardiac events (MACE [cardiac death, coronary artery bypass graft, acute myocardial infarction, stent thrombosis based on Academic Research Consortium definitions of definite/probable (17), target vessel revascularization and target lesion revascularization]) were assessed by office visits or by phone calls at 9-month follow-up.

Statistical methods. All statistical analyses were performed using SAS (v.9.2) software (SAS Institute, Cary, NC) and statistical significance was assessed at the 0.05 level. Continuous variables are expressed as mean \pm SD, and categorical variables are expressed as counts and percentages. For major segments and 2.5 mm sub-segment analyses, differences between time points, distinct baseline rates of malapposition (i.e. “Low” and “High” group), as well as differences observed between each group (DIS vs. BIF vs. BODY) were evaluated using generalized estimating equations (GEE) with exchangeable correlation to account for the clustering of values within each subject after adjusting for stent types. To estimate differences at frame level, multilevel mixed model, which can address random effects at segment and subject levels were used for binary and continuous outcomes comparisons. Mixed effects model was used to estimate correlation coefficient between malapposed struts percentage and mean lumen area at post-PCI with repeated observations.

Results

Patient characteristics and image acquisition.

All 33 patients underwent angiography and FD-OCT post-PCI and at 9-month (mean 286 ± 49.8 days) follow-up. Baseline clinical characteristics are reported in Table 1 and angiographic and procedural characteristics are shown in Table 2. No complications were identified. Most patients underwent kissing-balloon technique, followed by in-stent post-dilation in the BODY segment. Eleven patients were treated with SES and twenty-two patients were treated with EES. We planned a single stent strategy to treat all the cases; nevertheless, in 5 patients we had to use an additional stent in the proximal LAD, distal to the ULM stent, due to distal stent edge

dissections, while in 5 patients a second stent was required due to the long length of the diseased segment. One patient at post-PCI and two patients at 9-month follow-up had inadequate DIS segment stent evaluation due to incomplete FD-OCT pullback imaging. These segments (not the patients) were excluded from analysis.

FD-OCT findings

A total of 25,873 stent struts were analyzed. Post-PCI, progressively larger stent and lumen areas were identified in DIS, BIF, and BODY segments, respectively (Table 3). At 9-month follow-up, while stent areas remained unchanged compared to post-PCI, lumen areas were significantly reduced, preserving the differences between the segments (Table 3). Percentage of uncovered stent struts at 9 months was significantly different between each segment (DIS 3.4%, BIF 11.7%, and BODY 18.7%, $p < 0.05$ for all the comparisons).

Acute malapposition was significantly more common in BODY and BIF compared with DIS segment (Table 3, Figure 2). Significant reduction in percentage of malapposed stent struts was observed at 9-month follow-up in all segments (Table 3, Figure 3); however, while comparable low rates of malapposition were demonstrated in BIF (0.6%) and DIS (2.0%), significantly higher rates were observed in BODY (5.3%) segment (Table 3). The temporal evolution of stent strut malapposition is represented in Figure 4. NIH thickness of BIF segment was significantly higher than DIS and BODY segments, while NIH areas were comparable between the groups. There were no thrombus related to uncovered or malapposed stent struts at 9 month follow-up (Table 3).

When EES and SES were compared, similar rates of acute malapposition were observed in BODY and DIS segments, whereas significantly higher rates of malapposition were demonstrated in BIF segments treated with SES (Supplemental Table 1). At 9-month follow-up, a trend towards higher rates of malapposition with SES compared with EES was also observed in DIS and BIF segments. In addition, significantly higher rates of uncovered struts were observed in DIS segments treated with SES vs. EES and the same trend was observed in BIF

and BODY segments. Conversely, there was more NIH after EES compared with SES.

(Supplemental Table 2).

The impact of acute stent strut malapposition in stent-vessel interactions at 9-month follow-up was evaluated. The percentage of uncovered stent struts was significantly reduced in the “Low” compared with “High” group in DIS and BODY segments, with the same trend in BIF segment (Figure 5). Somewhat expected, 9-month malapposition rates and areas were higher in “High” compared to “Low” group in BODY segment, while similar trend was demonstrated in BIF and DIS segments. There was no impact of acute malapposition in the magnitude of NIH proliferation in DIS segment, whereas significantly reduced NIH area leading to less percentage stenosis was shown in BODY, with similar trend in BIF segment (Table 3, Figure 5). Figure 6 shows the representative acute malapposed stent struts at post-PCI which was persisted as uncovered malapposed stent struts at 9-month follow-up (Figure 6-C/D). We also made a reconstruction of 3D FD-OCT images of pullback at post-PCI (Figure 6-E/F) and 9-month follow-up (Figure 6-I/J).

Clinical Outcomes

All patients were taking dual antiplatelet therapy at 9-month follow-up. Target lesion revascularization occurred in 2 patients due to in-stent restenosis (ISR) and in 1 patient due to lesion progression in the LAD. There was no additional adverse cardiac event (Table 4).

Discussion

The present study provides novel FD-OCT insights on acute and late outcomes of DES implantation in lesions involving ULM bifurcation. The main observations were as follows: 1) In spite of modern high pressure balloon inflation techniques, stent malapposition remains a common phenomenon immediately post DES implantation in ULM, likely due to disproportionate larger sizes of left main BODY when compared to stent sizes available, leading to stent undersizing; 2) Acute and late DES-vessel interactions vary among different segments of ULM (DIS, BIF, and BODY) and stent type; 3) Stent malapposition in ULM is mostly

associated with decreased neointimal proliferation, without apparent increase in thrombus formation; 4) SES is associated with higher percentage of malapposition and uncovered struts compared with EES in ULM.

Substantial advancements in techniques and devices, as well as in adjunctive pharmacology, have led to an increase in PCI as a treatment of obstructive atherosclerotic disease in ULM (3). However, ULM remains a “high-risk” anatomical setting, in which stent thrombosis (ST) and/or restenosis can be catastrophic (18-21). The rationale for assessing DES-vessel interactions by means of a high-resolution intravascular imaging modality in vivo as surrogate for DES safety was primarily based on post-mortem studies, which suggested that delayed healing, inflammation, and malapposition were associated with ST (22). Intravascular OCT enables strut-level assessment of coverage and malapposition in vivo with high accuracy (6, 9, 16, 23-24). A recent OCT study showed that uncovered and malapposed stent struts, as well as their heterogeneous distribution along the stented segment, were more common in patients with compared to those without ST (25). Therefore, the assessment of DES-vessel interactions in different segments of ULM could play an important role to better understanding mechanisms of stent failure in this scenario. We recently demonstrated the safety and feasibility of evaluating ULM with FD-OCT compared to intravascular ultrasound (26). In the present study, we showed that larger segments of ULM had higher rates of uncovered stent struts (i.e., DIS<BIF<BODY). Despite marked improvement in malapposition rates compared to post-PCI in all segments of ULM (Figure 3), larger vessel segments remained with higher percentages and areas of stent strut malapposition at 9-month follow-up (Table 3, Figure 4). Indeed, malapposition rates and volumes were larger than previously observed in non-ULM setting (27).

The division of the stented segment in 2.5mm sub-segments enabled us to demonstrate that in-stent regions with high- compared to those with low-percentages of malapposition post-PCI had greater impact on vascular response at 9-month follow-up (Figure 5). These effects were more pronounced in the largest segment of ULM (i.e., BODY segment), in which neointimal

proliferation might not have been sufficient to cover stent struts adequately and to promote resolution of malapposition at 9-month follow-up. Similar observations were recently reported for non-ULM lesions (28). To our knowledge, this is the first intravascular imaging observation of acute DES malapposition and its impact in DES-vessel interactions at follow-up in lesions involving ULM bifurcation. Although all the procedures included in our study were conducted by experienced operators in a high-volume PCI center (1800 PCI/year, 180 left main PCI/year) and in-stent post-dilations with non-compliant balloons at high pressures were performed in 90.9% of the cases, acute malapposition rates identified by FD-OCT seemed relatively high, mostly in BIF and BODY segments. Therefore, we were able to identify, by means of high-resolution intravascular imaging (29), significant room for improvement in the technique of DES implantation in ULM (i.e., using larger stents, and/or larger balloons for post-dilation in larger segments). This seems particularly important as there is increasing evidence linking late stent malapposition (persistent and acquired) to late and very late ST (30). Whether FD-OCT guidance can improve ULM PCI acute results and long-term outcomes is yet to be determined, as PCI procedures in our study were not FD-OCT-guided; hence, additional interventions (i.e., post-dilation with higher pressure or larger balloons) based on FD-OCT information were not performed.

In spite of the demonstration of higher rates of uncovered and malapposed stent struts in larger segments of ULM, no thrombus or clinical evident ST were identified in our series at 9-month follow-up. However, our small sample size does not allow meaningful conclusions regarding such a rare adverse event. Finally, it is known that coronary bifurcations are more prone to develop ISR than non-bifurcated lesions (31), likely due to regions of low shear stress and different flow patterns (32). We demonstrated for the first time different degrees of NIH proliferation in distinct segments of ULM with higher NIH thickness in BIF compared to BODY and DIS segments. It is important to stress, however, that NIH area (which was comparable between different segments) rather than NIH thickness was our secondary,

previously specified endpoint; therefore, although an interesting finding, the difference demonstrated in the latter should be considered explorative. Future validation of our findings is warranted.

Conclusion.

The present study demonstrates the distinct patterns of DES-vessel interactions in different segments, DIS, BIF and BODY of ULM. Furthermore acute stent strut malapposition affects the DES-vessel interactions.

Study limitations. We were able to demonstrate for the first time vascular response after the implantation DES in ULM by means of high-resolution imaging; however, this pilot study was designed to provide seminal insights on ULM PCI with DES to be explored in future large trials. Hence, the relative small sample size precludes definitive conclusions regarding clinical outcomes. Incomplete blood clearance at ULM ostium might impair adequate FD-OCT assessments, nevertheless, we have demonstrated previously that only a very short segment of ostial ULM is affected (26). This paper includes only a population with lesions involving distal ULM; therefore, while this is the most prevalent situation in clinical practice, the results should not be extrapolated to lesions located in ULM shaft and ostium.

References

1. Mehilli J, Kastrati A, Byrne RA, et al. Paclitaxel- versus sirolimus-eluting stents for unprotected left main coronary artery disease. *J Am Coll Cardiol.* 2009;53:1760-1768.
2. Capodanno D, Stone GW, Morice MC, Bass TA, Tamburino C. Percutaneous coronary intervention versus coronary artery bypass graft surgery in left main coronary artery disease a meta-analysis of randomized clinical data. *J Am Coll Cardiol.* 2011;58:1426-1432.

3. Levine GN, Bates ER, Blankenship JC, et al. 2011 ACCF/AHA/SCAI Guideline for percutaneous coronary intervention: executive summary: a report of the American College of Cardiology Foundation/American Heart Association task force on practice guidelines and the Society for Cardiovascular Angiography and Interventions. *Circulation*. 2011;124:2574-60.
4. Chieffo A, Park SJ, Meliga E, et al. Late and very late stent thrombosis following drug-eluting stent implantation in unprotected left main coronary artery: a multicentre registry. *Eur Heart J*. 2008;29:2108-15.
5. Murata A, Wallace-Bradley D, Tellez A, et al. Accuracy of optical coherence tomography in the evaluation of neointimal coverage after stent implantation. *J Am Coll Cardiol Img*. 2010;3:76-84.
6. Guagliumi G, Sirbu V, Bezerra H, et al. Strut coverage and vessel wall response to zotarolimus-eluting and bare-metal stents implanted in patients with ST-segment elevation myocardial infarction: the OCTAMI (Optical Coherence Tomography in Acute Myocardial Infarction) study. *J Am Coll Cardiol Interv*. 2010;3:680-7.
7. Guagliumi G, Bezerra HG, Sirbu V, et al. Serial assessment of coronary artery response to paclitaxel-eluting stents using optical coherence tomography. *Circ Cardiovasc Interv*. 2012;5:30-38.
8. Guagliumi G, Musumeci G, Sirbu V, et al. Optical coherence tomography assessment of in vivo vascular response after implantation of overlapping bare-metal and drug-eluting stents. *J Am Coll Cardiol Interv*. 2010;3:531-9.
9. Douglas JS Jr, Holmes DR Jr, Kereiakes DJ, et al. Coronary stent restenosis in patients treated with cilostazol. *Circulation*. 2005;112:2826-32.
10. Van der Zwet PM, Reiber JH. A new approach for the quantification of complex lesion morphology: the gradient field transform; basic principles and validation results. *J Am Coll Cardiol*. 1994;24:216-224.

11. Bezerra HG, Costa MA, Guagliumi G, Rollins A, Simon D. Intracoronary optical coherence tomography: a comprehensive review. *J Am Coll Cardiol Interv.* 2009;2:1035-1046.
12. Mehanna EA, Attizzani GF, Kyono H, Hake M, Bezerra HG. Assessment of coronary stent by optical coherence tomography, methodology and definitions. *Int J Cardiovasc Imaging.* 2011;27: 259-269.
13. Moore P, Barlis P, Spiro J, et al. A randomized optical coherence tomography study of coronary stent strut coverage and luminal protrusion with rapamycin-eluting stents. *J Am Coll Cardiol Interv.* 2009;2:437-44.
14. Kume T, Akasaka T, Kawamoto T, et al. Assessment of coronary arterial thrombus by optical coherence tomography. *Am J Cardiol.* 2006;97:1713-7.
15. Bouma BE, Tearney GJ, Yabushita H, et al. Evaluation of intracoronary stenting by intravascular optical coherence tomography. *Heart.* 2003;89:317-20.
16. Cutlip DE, Windecker S, Mehran R, et al. Clinical end points in coronary stent trials: a case for standardized definitions. *Circulation.* 2007;115:2344-51.
17. Daemen J, Wenaweser P, Tsuchida K, et al. Early and late coronary stent thrombosis of sirolimus-eluting and paclitaxel-eluting stents in routine clinical practice: data from a large two-institutional cohort study. *Lancet.* 2007;369:667–78.
18. Lagerqvist B, James SK, Stenestrand U, Lindbäck J, Nilsson T, Wallentin L. Long-term outcomes with drug-eluting stents versus bare-metal stents in Sweden. *N Engl J Med.* 2007;356:1009–19.
19. Stone GW, Moses JW, Ellis SG, et al. Safety and efficacy of sirolimus- and paclitaxel-eluting coronary stents. *N Engl J Med.* 2007;356:998 –1008.
20. Pfisterer M, Brunner-La Rocca HP, Buser PT, et al. Late clinical events after clopidogrel discontinuation may limit the benefit of drug-eluting stents: an

- observational study of drug-eluting versus bare-metal stents. *J Am Coll Cardiol*. 2006;48:2584 –2591.
21. Finn V, Joner M, Nakazawa G, et al. Pathological correlates of late drug-eluting stent thrombosis - strut coverage as a marker of endothelialization. *Circulation*. 2007;115:2435-2441.
 22. Guagliumi G, Ikejima H, Sirbu V, et al. Impact of drug release kinetics on vascular response to different zotarolimus-eluting stents implanted in patients with long coronary stenoses: the LongOCT study (Optical Coherence Tomography in Long Lesions). *J Am Coll Cardiol Interv*. 2011;4:778-85.
 23. Guagliumi G, Costa MA, Sirbu V, et al. Strut coverage and late malapposition with paclitaxel-eluting stents compared with bare -metal stents in acute myocardial infarction: optical coherence tomography substudy of the harmonizing outcomes with revascularization and stents in acute myocardial infarction (HORIZONS-AMI) trial. *Circulation*. 2011;123:274-281.
 24. Guagliumi G, Sirbu V, Musumeci G, et al. Examination of the in vivo mechanisms of late drug-eluting stent thrombosis: findings from optical coherence tomography and intravascular ultrasound imaging. *J Am Coll Cardiol Interv*. 2012;5:2-20.
 25. Fujino Y, Bezerra HG, Attizzani GF, et al. Frequency-domain optical coherence tomography assessment of unprotected left main coronary artery disease - a comparison with intravascular ultrasound. *Catheter Cardiovasc Interv*. 2013; “Epub”.
 26. Guagliumi G, Capodanno D, Ikejima H, et al. Impact of different stent alloys on human vascular response to everolimus-eluting stent: An optical coherence tomography study: The OCTEVEREST. *Catheter Cardiovasc Interv*. 2012 Mar 16. [Epub].
 27. Gutiérrez-Chico JL, Wykrzykowska J, Nüesch E, et al. Vascular tissue reaction to acute malapposition in human coronary arteries: sequential assessment with optical coherence tomography. *Circ Cardiovasc Interv*. 2012;5:20-9.

28. Bezerra HG, Attizzani GF, Sirbu V, et al. Optical coherence tomography versus intravascular ultrasound to evaluate atherosclerosis and percutaneous coronary intervention. *J Am Coll Cardiol Interv* 2013;3:228-36.
29. Hassan A, Bergheanu S, Stijnen T, et al. Late stent malapposition risk is higher after drug-eluting stent compared to bare-metal stent implantation and associates with late stent thrombosis. *Eur Heart J*. 2010;31:1172-1180.
30. Carg S, Serruys PW. Coronary stents. Current status. *J Am Coll Cardiol*. 2010;56:S1-42.
31. Koskinas K, Chatzizisis Y, Antoniadis A, Giannoglou G. Role of endothelial shear stress in stent restenosis and thrombosis. Pathophysiologic mechanisms and implications for clinical translation. *J Am Coll Cardiol*. 2012;59:1337-1349.

Figure legends

Figure 1. Representative frequency-domain optical coherence tomography (FD-OCT) image and schema. Unprotected left main (ULM) was divided into three segments for the purpose of FD-OCT analyses, as follows: (1) Ostial-body (BODY), (2) Bifurcation (BIF), (3) Distal (DIS).

Brown line represents OCT catheter.

Figure 2. Relationship of malapposed struts percentage and mean lumen area (mm²) at post-PCI. Linear regression of malapposed struts percentage vs. mean lumen area (mm²) at post-PCI. Blue, red and green dots correspond respectively to DIS, BIF and BODY.

Figure 3. Time course of malapposed struts percentage after stent implantation. Percentage of malapposed struts at post-PCI and 9-month follow-up in DIS- (panel A), BIF- (panel B) and

BODY segments (panel C). Red dashed lines represent mean standard deviation of uncovered and malapposed struts percentage at each time point for BIF and ULM BODY segment.

Figure 4. Sub-segmental analysis of the temporal evolution of stent strut malapposition. Bar graphs depict number of sub-segments with malapposition (A, C, and E) and volumes of malapposition (B, D, and F) at post-PCI and 9-month follow-up. White bars represent acute and persistent malapposition at post-PCI and 9-month follow-up, respectively. Dark bars represent late acquired malapposition. Note that persistent, as well as late acquired malapposition assessments were based on the evaluation of co-registered sub-segments at post-PCI and 9 month follow-up.

Figure 5. Graph representation of the impact of baseline malapposition rates in vascular response at 9-month follow-up (F/U). Comparison of F/U frequency-domain optical coherence tomography assessments between two groups with different baseline malapposition rates (i.e., “Low” and “High” groups) in different major segments of unprotected left main (DIS, BIF, and BODY). Impact of malapposition at baseline in F/U uncovered struts percentage (A), malapposed struts percentage (B), neointimal hyperplasia (NIH) (C), malapposition area (D), NIH area (E) and percentage area stenosis are demonstrated (F).

Error bars represent \pm SEM; p value calculated by GEE model shows baseline malapposed struts percentage status fixed effects after adjustment of stent type

Figure 6. Uncovered and malapposed stent struts in unprotected left main (ULM) detection by two-(2-D) and three-dimensional (3-D) frequency-domain optical coherence tomography (FD-OCT) images post-PCI and at 9-month follow-up. Green, white and red Green, white, and red asterisks correspond, respectively, to upper left main (ULM) BODY, left circumflex artery, and left anterior descending artery. (A) Two-dimensional (2D) FD-OCT longitudinal view of post-PCI ULM is shown. The region highlighted by the white dashed line

corresponds to the cross section represented in (C); malapposed stent struts (white arrows) are depicted. The longitudinal view of the same region at 9-month follow-up demonstrates persistence of malapposed/uncovered stent struts (B), which can be better visualized in D (white arrows). (E) Three-dimensional (3D) reconstruction of the FD-OCT pullback is shown in A, in which malapposed stent struts are identified (white arrow). (F) The ULM is divided in 2 parts, which are represented as flattened images (G,H), showing uncovered stent struts after PCI.(I) A 3D reconstruction of the 9-month follow-up pullback is shown (B) and reveals persistence of malapposed/uncovered struts (white arrow). Note that when the image is divided in 2 parts (J), which are represented as flattened images (K,L), a heterogeneous pattern of stent coverage is demonstrated by higher rates of uncovered struts in BODY than in the left anterior descending artery (K)

Figure 1.

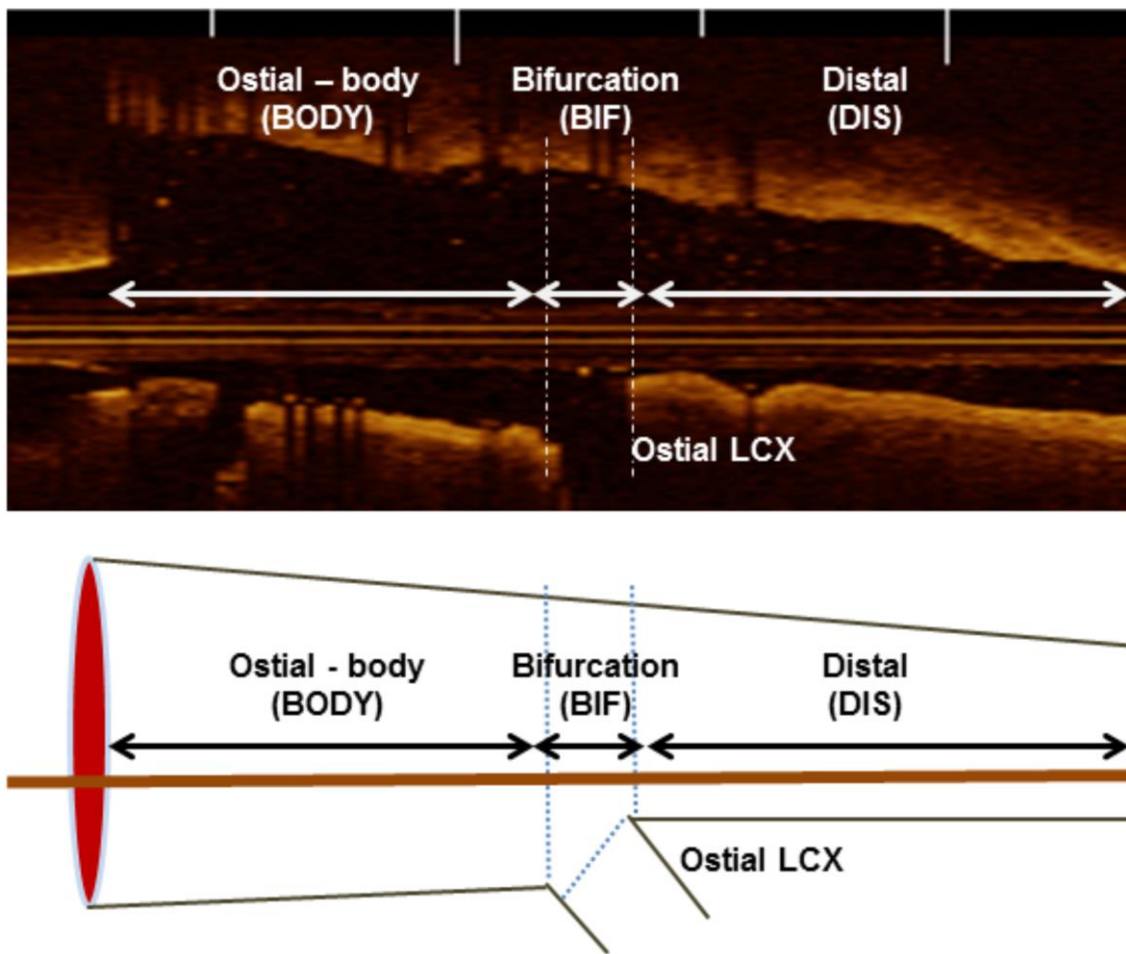


Figure 2.

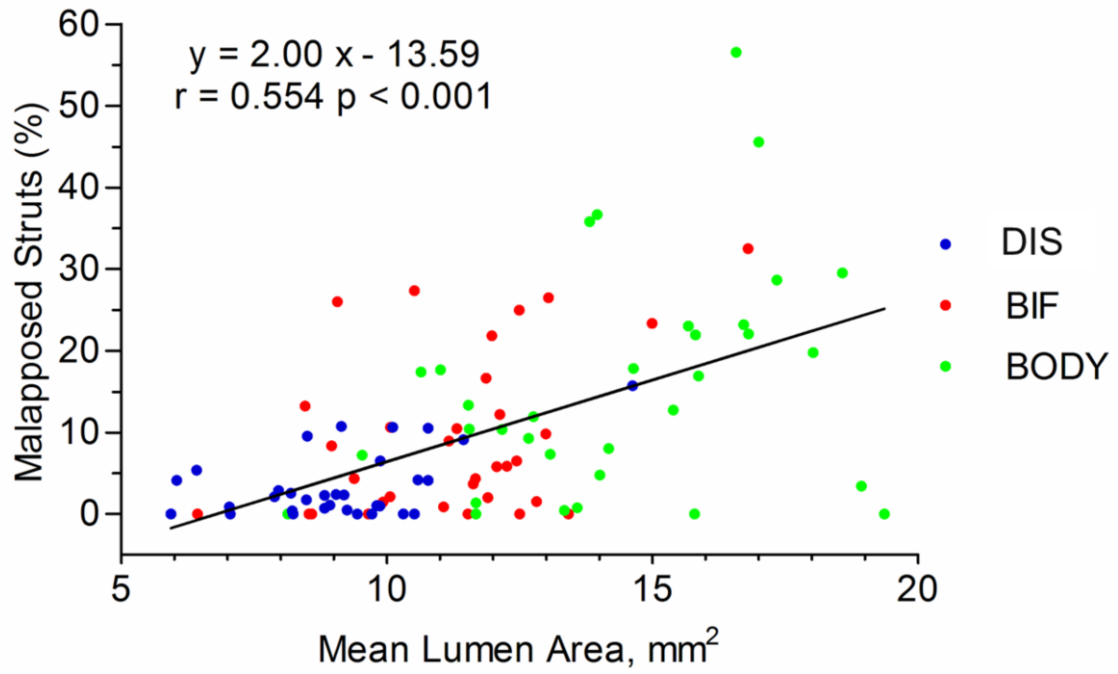


Figure 3.

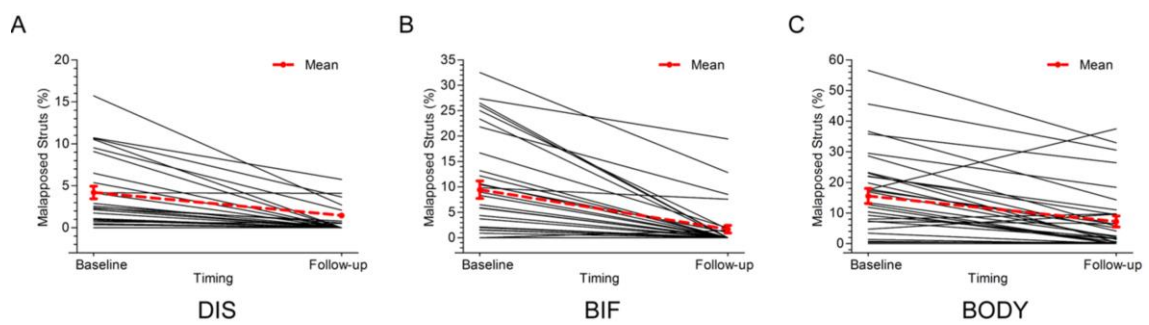


Figure 4.

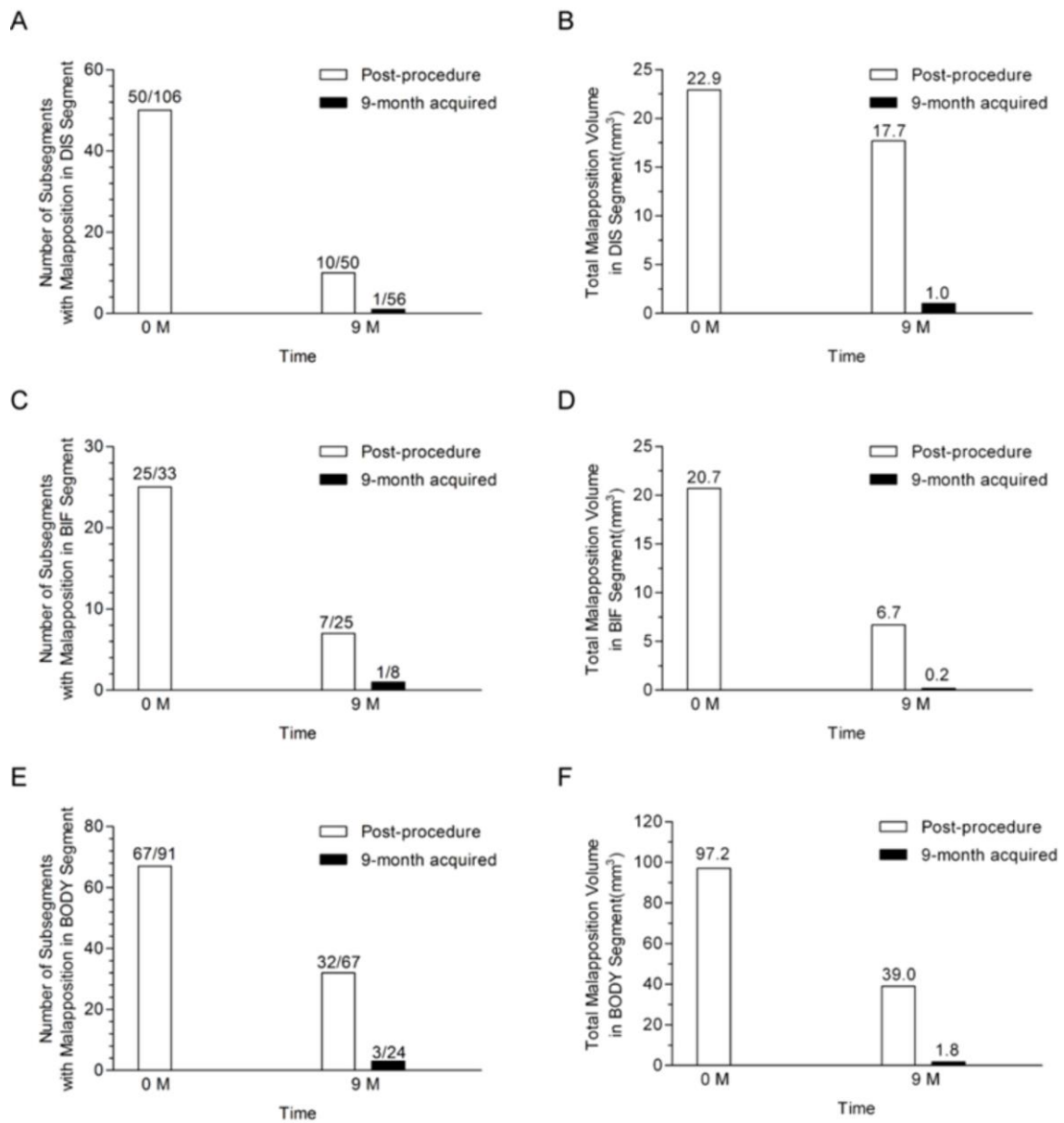


Figure 5.

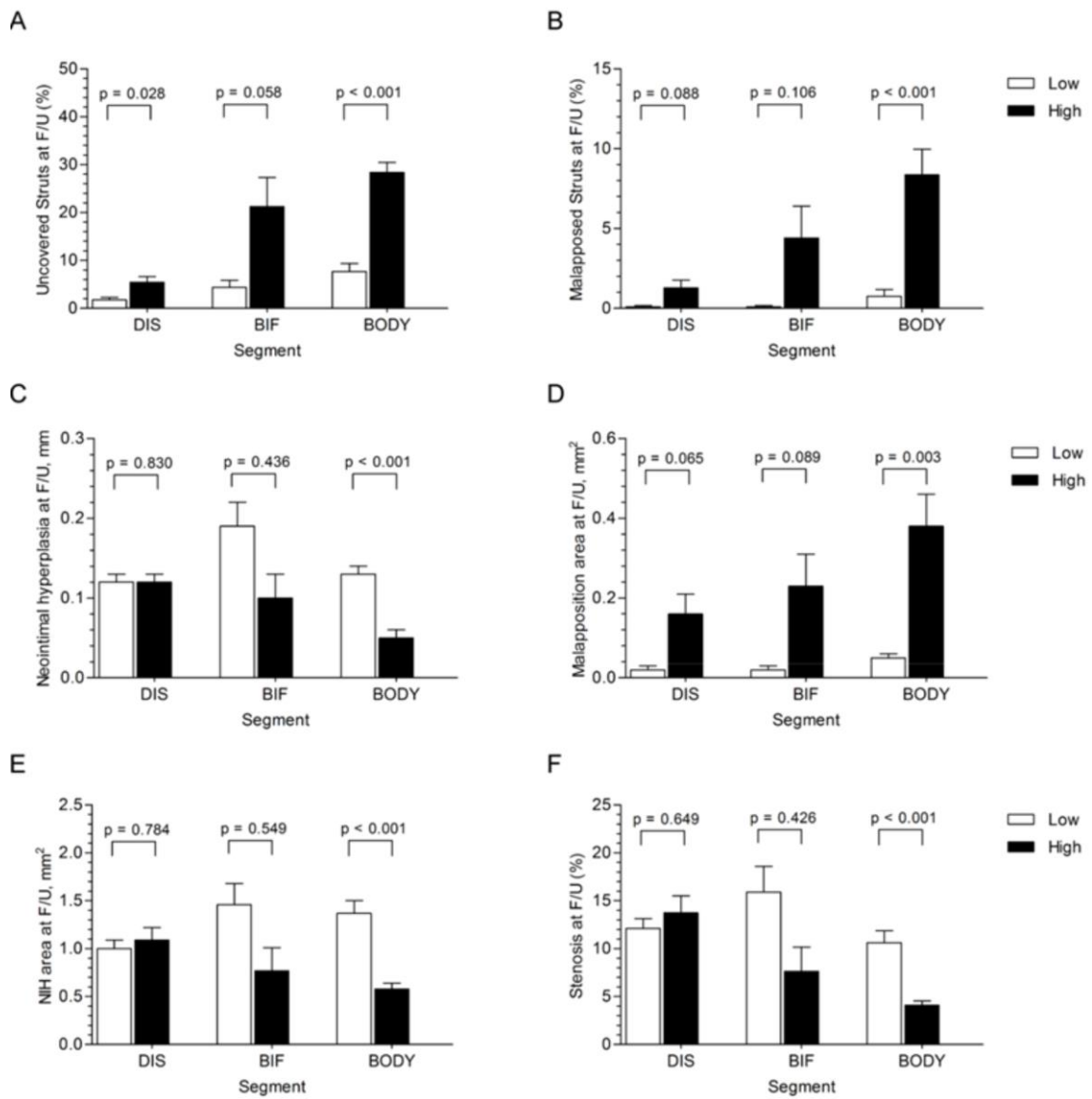


Figure 6.

